CORA Cork Open Research Archive
Cartlann Taighde Oscailte Chorcaí

Title	An open-source tool for the design and simulation of multilayer induction microcoils
Authors	O Donnell, Cian;Abomahmoud, Mohamed;Coombes, Sean Frank;Burke, Ray;O Hare, Daniel;Jaeger, Herman Alexander
Publication date	2026-09-25
Original Citation	O Donnell, C, Abomahmoud, M, Coombes, S F, Burke, R, O Hare, D & Jaeger, H A 2026, An open-source tool for the design and simulation of multilayer induction microcoils. in 2026 IEEE International Instrumentation and Measurement Technology Conference (I2MTC). Conference Record - IEEE Instrumentation and Measurement Technology Conference, Institute of Electrical and Electronics Engineers Inc., pp. 1-6, 2026 IEEE International Instrumentation and Measurement Technology Conference, I2MTC 2026, Nancy, France, 25/05/26. https://doi.org/10.1109/I2MTC66907.2026.11694655
Type of publication	Conference item
Link to publisher's version	https://www.scopus.com/pages/publications/105053010150 - 10.1109/I2MTC66907.2026.11694655
Rights	© 2026, IEEE. Personal use of this material is permitted. Permission from IEEE must be obtained for all other uses, in any current or future media, including reprinting/republishing this material for advertising or promotional purposes, creating new collective works, for resale or redistribution to servers or lists, or reuse of any copyrighted component of this work in other works.
Download date	2026-11-07 10:30:49
Item downloaded from	https://hdl.handle.net/10468/19552



University College Cork, Ireland
Coláiste na hOllscoile Corcaigh

An Open-Source Tool for the Design and Simulation of Multilayer Induction Microcoils

Cian O'Donnell
Tyndall National Institute
Cork, Ireland

Mohamed AboMahmoud
Tyndall National Institute
Cork, Ireland

Sean Frank Coombes
University College Cork
Cork, Ireland

Ray Burke
Tyndall National Institute
Cork, Ireland

Daniel O'Hare
Tyndall National Institute
Cork, Ireland

Herman Alexander Jaeger
Tyndall National Institute
Cork, Ireland

***Abstract*—Induction microcoils are valued for their simplicity, sensitivity, and cost effectiveness across a wide range of applications in biomedical instrumentation. The design of compact application-specific multilayer coils using permeable magnetic cores is a challenge that often requires multiple hardware iterations. This paper presents a simulation software tool for the evaluation of induction microcoil designs. Built upon the well known open-source Finite Element Method Magnetics software package, the tool allows users to rapidly simulate the magnetic and electrical characteristics of multilayer induction microcoils in response to a time-varying magnetic field. Simulated inductance, resistance and sensitivity measurements are acquired from the microcoil structures using a novel procedurally generated Helmholtz coil technique and ensures a uniform and homogenous flux density is applied to the microcoil under test. The tool is written in the python programming language and allows multiple simulations to be executed concurrently thus enabling the users to perform parameter sweeps of a coil design. The tool is validated against a set of custom induction microcoils with coil resistance, inductance and sensitivity simulated to within 3%, 22% and 11% of the experimentally measured values respectively. The tool is freely available on GitHub and PyPI software repositories.**

***Index Terms*—induction coil, microcoils, sensing, core, coil design, finite element analysis, python.**

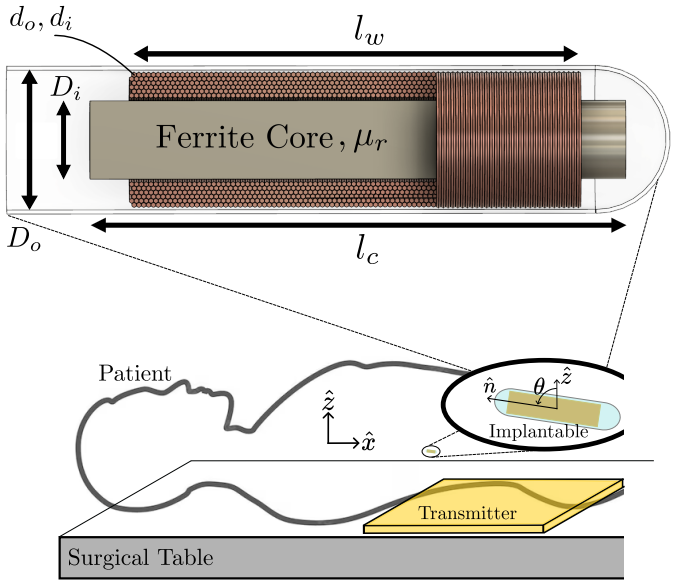


Fig. 1: An induction microcoil used in an implantable medical device with constraining geometries shown. Wire leads are not shown.

I. Introduction

Induction microcoils play an important role in biomedical applications including surgical navigation [1], deep brain stimulation [2], motion analysis [3], wireless capsule endoscopy [4] and wireless power transfer [5], [6]. Designing a coil to meet a particular application requirement can be a resource intensive process requiring engineering resources to be spent on developing an electrical model for a given set of mechanical constraints and application demands.

An illustration of a solenoidal microcoil used in an implantable medical device is shown in Fig. 1. Microcoils are typically manufactured using enamelled copper wire wound on a former or mandrel. A permeable magnetic core may be used to increase the magnetic flux density within the coil as is the case in electromagnetic tracking (EMT) where the induced voltage on a small microcoil is used to localise the position and orientation of surgical instruments [7]. The presence of a permeable core within the microcoil serves to maximise the induced voltage generated in the winding in the presence of a time-varying magnetic field [8]. Coils for wireless power transfer applications are also required to meet a predetermined inductance-to-resistance ratio to form a low loss, high quality factor (Q) coil that resonates and transfers power from a wireless power transmitter to a load [6].

Achieving a microcoil design to meet both the electrical and mechanical design constraints of a given application can be a challenging task. Prototyping microcoil designs is beyond the manufacturing capabilities of a typical electronics lab due to the small wire gauges and small geometries of the winding wire and magnetic cores. Commercial coil manufacturers can readily produce windings at very small dimensions, however this process becomes expensive and time-consuming if multiple design iterations are required. The objective of the coil designer is therefore to provide a manufacturer with a suitable mechanical design specification that meets the desired electrical specification for a given application. Determining

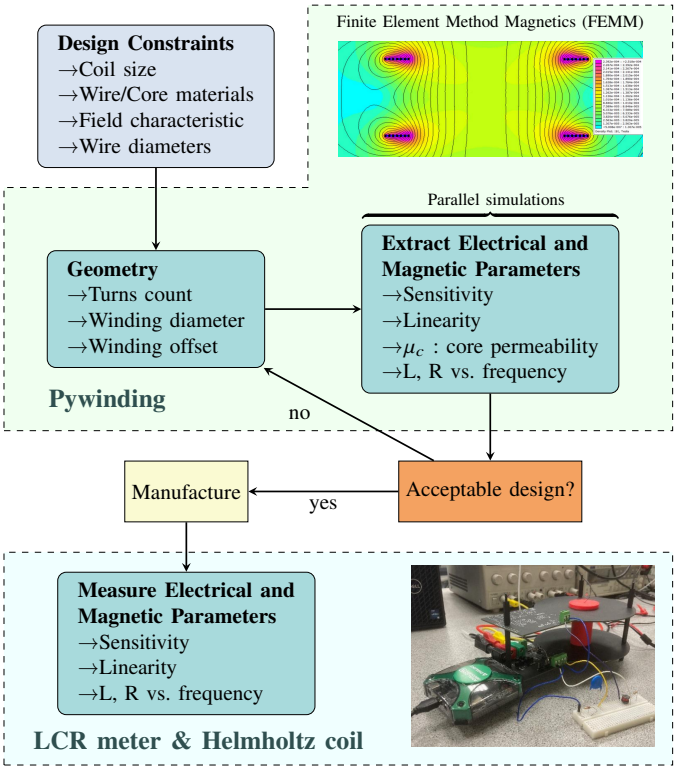


Fig. 2: Design flow for the Pywinding tool.

the electrical performance of a coil is typically performed using a calculator or simulation package where the mechanical dimensions of the microcoil are used as input to an analytical or finite element model. Coil64 [9] is a user-friendly free coil calculator software package that makes use of analytical expressions, such as Wheeler's formula [10] , to quickly estimate a microcoil's electrical parameters for a given winding geometry. However the analytical approximations it provides are limited and do not support the analysis of multilayer coils with permeable cores. Both free and commercial finite element simulation tools can be used to simulate more advanced geometries and materials. The Finite Element Method Magnetics (FEMM) [11] package is a well respected open-source tool and is capable of simulating a microcoil's magnetic and electrical responses represented as an axisymmetric magnetics problem. FEMM is a proven simulation tool and is commonly used in magnetics research, however the software package features an unconventional user interface. Advanced coil designs and iterative simulations of those designs can be achieved using FEMM's scriptable programming interface, pyFEMM [12], however the development associated with using this interface may not be feasible for the end user.

This work helps address the design problem by presenting an open-source simulation tool for the design and development of induction microcoils [13]. Pywinding follows the design flow shown in Fig. 2. Material and geometric specifications of a microcoil are accepted as input from the user as illustrated in Fig. 1 and detailed in Table I. A parallel sweep of

TABLE I: List of input parameters to the Pywinding tool.

Parameter	Description
D_o	Total diameter of the sensor
D_i	Outer diameter of sensor core only
d_o	Total diameter of magnet wire
d_i	Diameter of the magnetic wire copper
l_w	Length of the winding
l_c	Length of the core
material	The material of the permeable core
N	The number of turns on the winding

simulations is then executed using the FEMM [11] package. The tool returns key simulation outputs to the user including the sensitivity of the microcoil in units of $\mathrm{V\,T^{-1}\,Hz^{-1}}$ as well as simulated winding inductance and resistance values. A key consideration of the presented tool is its ability to characterise the effective magnetic permeability of the core, μ_e, and the effects of core saturation and demagnetisation [14]. Pywinding allows engineers to virtually prototype the magnetic and electrical properties of induction microcoil designs in a finite element simulation environment in order to inform the feasibility of a proposed microcoil geometry for a given application. The tool operates in the magneto-quasistatic (MQS) regime and does not model electric fields or capacitive effects, however the consequences of the skin and proximity effects are included in the model. Section II briefly discusses the physics of induction coils, section III then details the simulation stages of the software tool with respect to user inputs and outputs. Section IV and V compares and discusses the electrical parameters of simulations with experimental measurements from a set of custom manufactured microcoils.

II. Induction Microcoil Design

An induction microcoil will generate a time-varying voltage at its terminals when placed in a time-varying magnetic field. If the coil is placed in a time-varying magnetic field of uniform flux density, B, such that its axis is aligned with the direction of the field lines, then the voltage induced on the induction coil, $v(t)$, can be expressed using scalar notation and is solely a function of the applied magnetic flux density and the coil's mechanical and material parameters:

$$v(t) = -\mu_e N A \frac{dB(t)}{dt} \qquad \text{[V]} \quad (1)$$

where $B(t)$ is the amplitude of the applied magnetic flux density as a function of time, t, at the coil's location, in units of tesla, A is the cross-sectional area of the coil, N is the number of turns on the coil and μ_e is the resultant/effective relative permeability of the ferromagnetic core upon which the coil is wound, and will be discussed shortly. If a sinusoidal magnetic field of the form $B(t) = B\cos(\omega t)$ is applied to the sensor then the voltage on the sensor can be expressed in (2) as

$$v(t) = -(\mu_e N A 2\pi) f B \cos(\omega t) \qquad \text{[V]} \quad (2)$$

where $\omega = 2\pi f$ is the angular frequency of the sinusoidal reference waveform of frequency f, in hertz. The product of the five constants in parentheses in (2) represents the frequency-normalised sensitivity of the microcoil, S, and is defined in units of volts per tesla per hertz:

$$S = \mu_e N A 2\pi \qquad [\mathrm{V\,T^{-1}\,Hz^{-1}}] \quad (3)$$

The minute cross-sectional area of microcoils results in a low intrinsic sensitivity unless a ferromagnetic core is used. Ferromagnetic cores boost the magnetic flux density within the coil, and thus the induced voltage $v(t)$, by acting as a magnetic flux concentrator. While ferromagnetic cores enhance the sensitivity of a coil, the degree to which flux concentration occurs is determined by the shape of the core. The expression for a core's effective relative permeability, μ_e is given by:

$$\mu_e = \frac{\mu_r}{1 + N_d \cdot (\mu_r - 1)} \quad (4)$$

where μ_r is the relative permeability of the bulk material and N_d is the demagnetizing factor and is a function of the aspect ratio of the core [14]. Values of N_d and thus μ_e can be approximated using analytical formulations for ellipsoidal core geometries [15] however finite element methods are better suited for assessing the magnetic response of arbitrary core geometries. The presented tool facilitates the analysis of the demagnetizing effect, as well as skin effects, proximity effects and the effects of core saturation.

III. Simulation Methods

The Pywinding tool executes a simulation in 7 steps:

1) The user submits a list of coil geometry parameters as illustrated in Fig. 1 consisting of width and length of the desired microcoil and the core. The core material and winding wire parameters are also specified. A number of desired test flux densities, M, and a stimulus frequency f, in hertz, for the simulation are also provided. The B-H curves of arbitrary materials can be manually loaded into FEMM using the *Materials Library* feature.
2) The tool generates the maximum number of winding wire turns, $n_{\max}$, that can possibly fit within the user-provided geometry and calculates the total number of feasible winding layers. The user is free to override the turn count parameter to reflect any additional mechanical constraints not captured by the tool.
3) The tool uses the pyFEMM scripting interface [12] to generate an axisymmetric magnetic problem within the Finite Element Method Magnetics program. In addition, the tool defines the geometry of a single-axis Helmholtz coil array whose radial dimensions are 100× the largest dimension of the microcoil. The Helmholtz array is used to generate a homogenous magnetic field in the vicinity of the microcoil as shown in Fig. 3.
4) Multiple `.fem` project files are generated by the tool with each simulation file configured to apply a predetermined flux density at the microcoil location. The effectiveness of a particular core material is calculated by comparing the microcoil's electrical response with its air-cored alternative. Thus there will be $2M$ project files generated for a testing range of M stimulus flux densities. The required stimulus current for the Helmholtz coil array, I_H, that is necessary for a given applied flux density within the bore of the array, B_H, is calculated by rearranging the well known analytical expression for the flux density within the centre the array [16]:

$$B_{\mathrm{H}} = \left(\frac{4}{5}\right)^{1.5} \frac{\mu_0 n I_H}{R} \qquad [\mathrm{T}] \quad (5)$$

where B_H is one of M test flux densities, $n = 1$ is the modelled number of turns on the Helmholtz coil, R is the radius of the Helmholtz coil and $\mu_0 = 4\pi \times 10^{-7}$ is the freespace magnetic permeability.
5) Each `.fem` file is simulated by the host machine. Simulation speed is accelerated with the use of python's multiprocessing features via the `concurrent.futures` module of the standard library. Each `.fem` project file is simulated in a dedicated instance of the FEMM software package where the number of simulation instances is equal to the number of CPU cores on the host system. The simulated responses of the microcoil are collated into a data structure and returned to the user.
6) One final simulation is executed to extract the inductance L and resistance R of the microcoil and is performed by simulating a small alternating current of 1 µA through the microcoil and recording the circuit parameters reported by FEMM.
7) The acquired data are printed and plotted to the host computer screen. The simulation data are saved to a `.mat` file for easy compatibility with Matlab for plotting and further analysis.

The steps described above can be executed as a single script or can be executed step-by-step in an interactive python interpreter session.

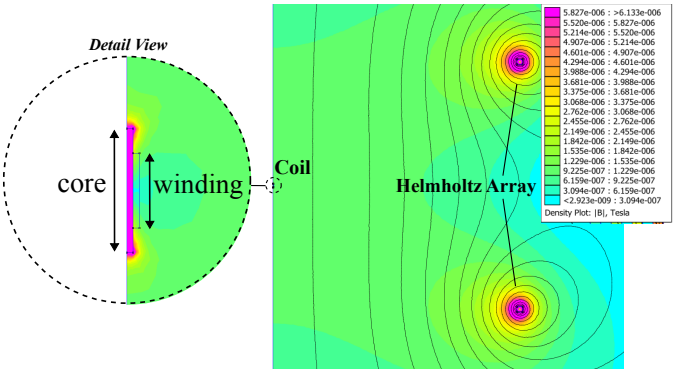


Fig. 3: Axisymmetric FEMM solution of an induction microcoil experiencing a 1 µT flux density generated by a single-axis Helmholtz array. Temperature map regions of high flux density are shown in purple.

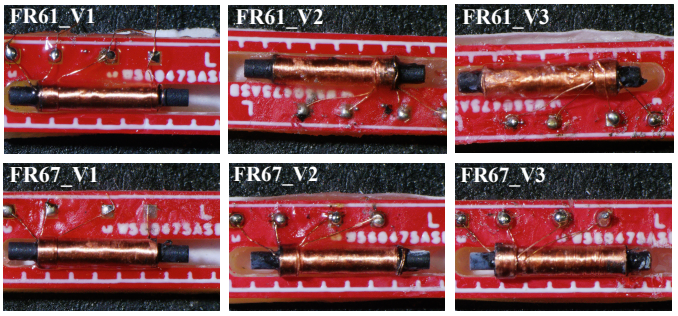


Fig. 4: Microscope images of the realised coil designs which were simulated. Coils are wound on Fair-Rite FR61 and FR67 ferrite rods.

IV. Experimental & Simulated Results

The simulation performance of the tool was validated by comparing simulated results with corresponding measurements acquired for a set of six custom induction coil designs shown in Fig. 4. The mechanical input parameters for these coils as shown in Table I are given in Table II . The designs were manufactured by a coil winding company (*KUK Electronic AG, Appenzell, Switzerland*) using commercially available self-bonding magnet wire *(Elektrisola GmbH, Eckenhagen, Germany)*. The coil designs utilised commercially available FR67 and FR61 ferromagnetic cores (Fair-Rite, NY, USA). The magnetic characteristics of these cores was defined in FEMM in the *Materials Library* using the B-H curve data obtained from material datasheets provided by the manufacturer.

The Pywinding simulation tool was initialised with the mechanical parameters of the manufactured microcoils. A magnetic field stimulus setting of 1 µT at a frequency of 1 kHz was used. The results of the simulated and corresponding measured electrical results are shown in Table II. The corresponding FEMM solution file is shown in Fig. 3.

Measured electrical resistance and inductance measurements were acquired using a model 895 LCR meter *(BK Precision, Yorba Linda, CA, USA)*, while sensitivity measurements were measured using a custom single-axis Helmholtz array driven by a closed-loop current source circuit based on the work of [8]. The Helmholtz array was calibrated with a GM08 gaussmeter *(Hirst Instruments, Falmouth, UK)*. The signed percentage errors between the simulated and measured results are calculated as Error = $(P_{\text{sim}} - P_{\text{meas}})/P_{\text{meas}} \times 100\%$.

A swept simulation between 1 µT and 50 µT with $M = 10$ points was performed on the FR61_V1 sensor variant whose results are shown in Fig. 5. The linear fit of the data gives a slope of 50.19 V T^{-1}. Normalisation with respect to the test frequency f of 1 kHz yields a sensitivity value of $S = 0.0519$ $\text{V T}^{-1}\,\text{Hz}^{-1}$ which aligns with the corresponding measured value in Table II.

A larger swept simulation was performed on the FR61_V1 microcoil ranging from 1 µT to 3 mT with a total of $M = 100$ simulation points. The resulting data in Fig. 6 shows the non-linear behaviour of the core as the slope begins to decrease for an excitation field of approximately 1 mT.

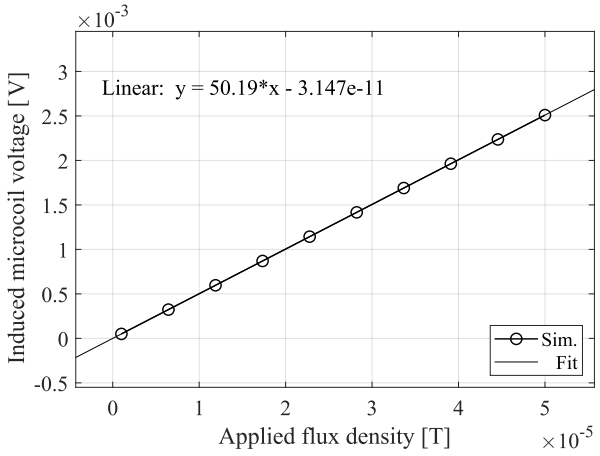


Fig. 5: Induced voltage on the FR61_V1 microcoil for applied fields between 1 µT and 50 µT.

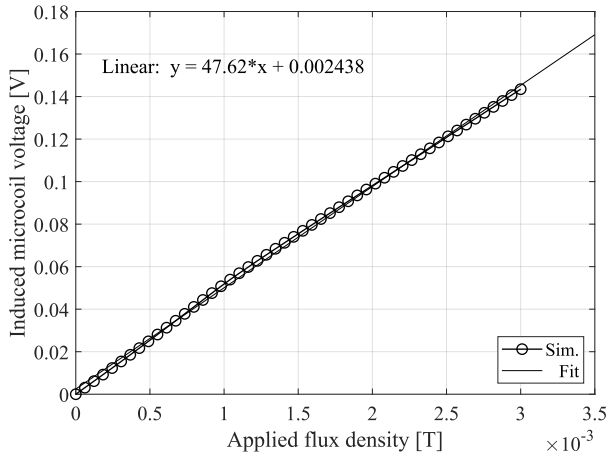


Fig. 6: Induced voltage on the FR61_V1 microcoil for applied fields between 1 µT to 3 mT @ f = 1 kHz. The sensitivity of the microcoil drops as the core begins to saturate.

The corresponding effective permeability μ_e for this simulated dataset is plotted as a function of the applied flux density in Fig. 7. The initial, maximum and saturation permeability regions of the plot are shown. For applied flux densities below 0.1 mT the value of μ_e remains constant with a value of approximately 33. Beyond 1 mT the effective permeability drops due to core material of the sensor beginning to saturate.

TABLE II: Mechanical and electrical characteristics of the manufactured coils. Simulated and measured electrical parameters were obtained at a stimulus frequency of 1 kHz. Both FR61 and FR67 cores both have lengths l_c = 7.5 mm and diameter D_i = 0.75 mm. The length of the winding upon the cores l_w = 5.5 mm.

Microcoil	d_i	N	**Layers**	**Total** N	**Simulated**			**Measured**			**Error**		
					R	L	S	R	L	S	ΔR	ΔL	ΔS
	[um]	[turns]	[layers]		[Ω]	[μH]	[$\mathrm{V\,T^{-1}\,Hz^{-1}}$]	[Ω]	[μH]	[$\mathrm{V\,T^{-1}\,Hz^{-1}}$]	[%]	[%]	[%]
FR67_V1	43	83	5	415	17.52	467.1	0.0299	17.32	574.7	0.0336	1.14	-18.72	-10.77
FR67_V2	50	72	4	288	8.99	217.5	0.0205	8.964	258.2	0.0231	0.29	-15.76	-10.97
FR67_V3	40	90	6	540	26.38	725.3	0.0388	26.29	922.5	0.0434	0.34	-21.38	-10.6
FR61_V1	43	83	5	415	17.52	766.5	0.0501	17.14	860.2	0.0465	2.22	-10.89	7.74
FR61_V2	50	72	4	288	8.99	356.7	0.0342	8.909	407.0	0.0323	0.91	-12.36	5.88
FR61_V3	43	90	6	540	26.38	1196	0.0640	26.12	1411	0.0633	1.00	-15.24	1.11

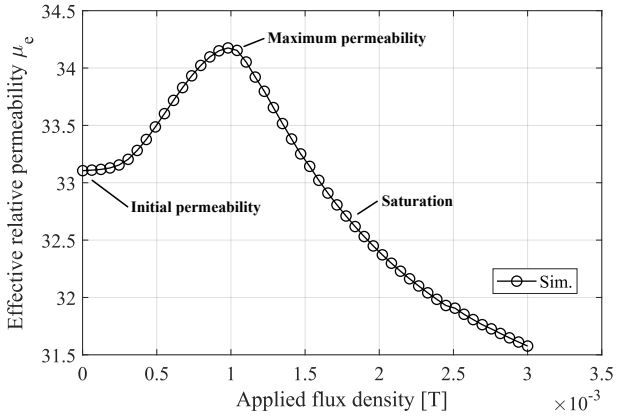


Fig. 7: Effective magnetic permeability μ_e of the FR61_V1 core for applied fields between 1 μT and 3 mT at f = 1 kHz. Core saturation begins to occur for applied flux densities above 1 mT.

V. Discussion

A comparison of the simulated and measured results for the manufactured induction coils is shown in Table II. The simulated winding resistance values closely align with measured values to within a 1-2%. Simulated inductance values consistently underestimate the true inductance by about 10-20%. Sensitivity estimates differ by at most 11%. These variances can be attributed to core material variability, stray lead wire inductances, the imperfect symmetry of the coil's physical windings as well as the consequences of simulation approximations made within the FEMM simulation environment which are not an accurate reflection of the manufactured coils.

This is exemplified by FEMM's approach to modelling windings, which uses a continuum model to represent regions of contiguous turns of magnet wire [17]. The approximation assumes perfect hexagonal packing of the copper magnet wire and does not account for any imperfections present in manufactured coil windings. The approximation is necessary due to the high number of turns on microcoils which can be in the order of 10^2 to 10^3. Otherwise, the complexity of modelling each individual wire turn would result in impractically large finite-element domain mesh. FEMM natively supports this continuum modelling approach which is detailed on p. 31 of the user manual [11] which also takes proximity and skin effects into account.

The plots shown in Fig. 6 and 7 show the performance of the FR61_V1 microcoil over a large range of applied flux densities. The normalised sensitivity of the microcoil based on linear fit of Fig. 6 is 47.62 $\mathrm{V\,T^{-1}\,Hz^{-1}}$ which is reduced compared to the sensitivity based on Fig. 5 where the sensitivity is 50.19 $\mathrm{V\,T^{-1}\,Hz^{-1}}$. Fig. 7 clearly shows the point at which core saturation begins to occur. A slight peaking is observed prior to saturation, which closely aligns with data presented in the manufacturer datasheet [18].

The presented Pywinding tool should be treated as a high-level tool for estimating the magnetic properties of microcoil designs. The results of the tool can be used to narrow the design space for a given application after which a more detailed simulation can be performed. A key limitation of this tool is its inability to determine a microcoil's self-capacitance. Simulation of a microcoil's capacitive effects and/or its full electrodynamic behaviour requires the modelling of a time-varying electric field which is beyond the scope of this tool, but can be achieved with well-known commercially available simulation packages.

VI. Conclusion

This work presenta Pywinding as a fast open-source tool for the design and evaluation of multilayer cored induction coils. The tool allows users to simulate low-frequency multilayer cored induction coils with good precision when given a set of microcoil dimensions. The tool's accuracy is verified against a set of custom induction microcoils for use in biomedical applications, however the tool can be used to simulate cylindrical coils of arbitrary size and aspect ratios. Uniform magnetic field stimuli are generated using a novel virtual Helmholtz array technique that scales with the dimensions of the sensor under test. The Pywinding tool is limited to solving the resistance, inductance and sensitivity properties of coils. Simulation of capacitive effects are beyond the scope of this tool and require more advanced finite element software packages. The tool does not require prior knowledge of FEMM or Python in order to be used effectively and will be a valuable resource for medical device researchers and manufacturing engineers. Future work on Pywinding will see further development of the package to incorporate additional coil geometries and parameter sweep

features. The tool is freely available on the Python package index (https://pypi.org/project/pywinding/).

ACKNOWLEDGMENT

This work is supported by Research Ireland grant 22/PATH-S/10867 and Health Holland LSHM-21058.

REFERENCES

[1] H. A. Jaeger, A. M. Franz, K. O'Donoghue, A. Seitel, F. Trauzettel, L. Maier-Hein, and P. Cantillon-Murphy, "Anser EMT: The first open-source electromagnetic tracking platform for image-guided interventions," *International Journal of Computer Assisted Radiology and Surgery*, vol. 12, no. 6, pp. 1059–1067, 2017.

[2] A. Khalifa, M. Zaeimbashi, T. X. Zhou, S. M. Abrishami, N. Sun, S. Park, T. Šumarac, J. Qu, I. Zohar, A. Yacoby, S. Cash, and N. X. Sun, "The development of microfabricated solenoids with magnetic cores for micromagnetic neural stimulation," *Microsystems & Nanoengineering*, vol. 7, no. 1, p. 91, Nov. 2021.

[3] H. Mohammadbagherpoor, P. Ierymenko, M. H. Craver, J. Carlson, D. Dausch, E. Grant, and J. D. Lucey, "An Implantable Wireless Inductive Sensor System Designed to Monitor Prosthesis Motion in Total Joint Replacement Surgery," *IEEE Transactions on Biomedical Engineering*, vol. 67, no. 6, pp. 1718–1726, Jun. 2020.

[4] Y. Fu, Y. Li, X. Wu, M. Liu, and Y.-X. Guo, "Wireless Electromagnetic Tracking System for Wireless Capsule Endoscope," *IEEE Transactions on Instrumentation and Measurement*, vol. 74, pp. 1–13, 2025.

[5] H. J. Sharemi, I. Habibagahi, R. P. Mathews, and A. Babakhani, "Robust Communication and Power Transfer over a Single Loosely Coupled Inductive Link for Miniaturized and Batteryless Sensing Devices," *IEEE Sensors Journal*, pp. 1–1, 2025.

[6] C. O'Donnell, H. A. Jaeger, R. Burke, and D. O'Hare, "Field Shaping for Enhanced Wireless Power Transfer in Misaligned Biomedical Inductive Links," in *2025 IEEE Wireless Power Technology Conference and Expo (WPTCE)*, Jun. 2025, pp. 1–4.

[7] H. A. Jaeger and P. Cantillon-Murphy, "Electromagnetic Tracking Using Modular, Tiled Field Generators," *IEEE Transactions on Instrumentation and Measurement*, vol. 68, no. 12, p. 8, 2019.

[8] H. A. Jaeger, K. O'Donoghue, and P. C. Murphy, "Induction sensor characterisation for electromagnetic tracking systems," in *2022 IEEE International Instrumentation and Measurement Technology Conference (I2MTC)*. Ottawa, ON, Canada: IEEE, May 2022, pp. 1–6.

[9] radioacoustick, "Coil64: inductance coil calculator," https://github.com/radioacoustick/Coil64, May 2025, version v2.3.35.

[10] H. Wheeler, "Inductance formulas for circular and square coils," *Proceedings of the IEEE*, vol. 70, no. 12, pp. 1449–1450, 1982.

[11] D. C. Meeker, "Finite element method magnetics (femm) homepage," 2025, [Online; accessed 26-May-2025]. [Online]. Available: https://www.femm.info/wiki/HomePage

[12] "pyFEMM – A Python Interface to FEMM:Finite Element Method Magnetics." [Online]. Available: https://www.femm.info/wiki/pyfemm

[13] H. A. Jaeger, C. O'Donnell, M. Abo Mahmoud, S. Coombes, R. Burke, and D. O'Hare, "PyWinding - A simulation tool for the design and evaluation of induction microcoils," Zenodo, Dec. 2025. [Online]. Available: https://doi.org/10.5281/zenodo.17793822

[14] S. Tumanski, "Induction coil sensors—a review," *Measurement Science and Technology*, vol. 18, no. 3, p. R31, 2007.

[15] J. A. Osborn, "Demagnetizing factors of the general ellipsoid," *Physical review*, vol. 67, no. 11-12, p. 351, 1945.

[16] R. Beiranvand, "Effects of the Winding Cross-Section Shape on the Magnetic Field Uniformity of the High Field Circular Helmholtz Coil Systems," *IEEE Transactions on Industrial Electronics*, vol. 64, no. 9, pp. 7120–7131, Sep. 2017.

[17] D. C. Meeker, "An improved continuum skin and proximity effect model for hexagonally packed wires," *Journal of Computational and Applied Mathematics*, vol. 236, no. 18, pp. 4635–4644, Dec. 2012.

[18] Fair-Rite, "61 Material™ Data Sheet," https://fair-rite.com/61-material-data-sheet/.